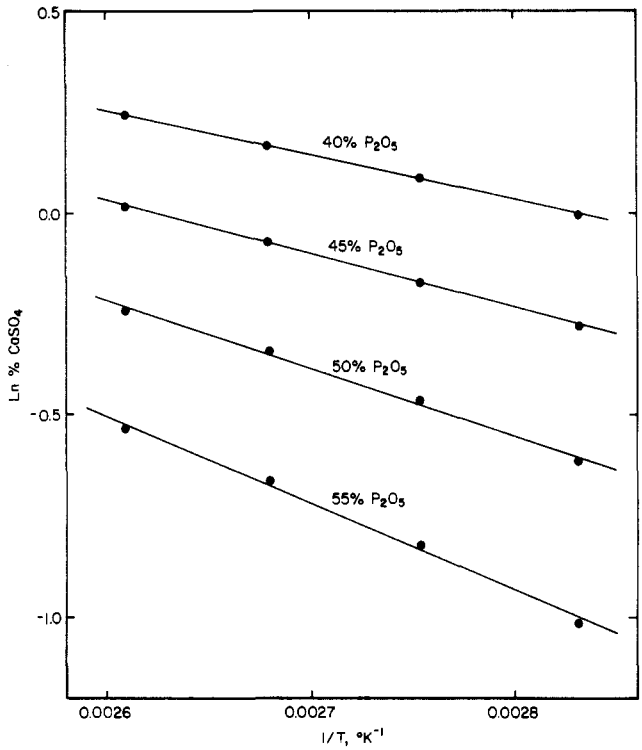

Figure 6. ln % $CaSO_4$ versus $1/T$ for 40, 45, 50, and 55% P_2O_5 solutions.

Table II. van't Hoff Parameters Associated with Weight Percent Saturation of α-$CaSO_4 \cdot 0.5H_2O$ in Concentrated Phosphoric Acid

% P_2O_5	ΔH, cal/mol	C	R^{2a}
40	2201.9 ± 19.1	3.135 ± 0.002	0.999
45	2648.2 ± 36.9	3.496 ± 0.003	0.999
50	3295.4 ± 70.9	4.092 ± 0.006	0.999
55	4307.7 ± 143.7	5.134 ± 0.012	0.998

[a] Correlation coefficient for fit of data to eq 3.

The solubility data also may be used to determine the apparent weight percent solubility product constants (column 6, Table I) for α-$CaSO_4 \cdot 0.5H_2O$ in concentrated phosphoric acid, as defined by the equation

$$K_{sp} = (\%\ Ca)(\%\ SO_4) = 0.20773(\%\ CaSO_4)^2 \quad (5)$$

Regression of the data in terms of temperature (t), °C, and P_2O_5 concentration (% P_2O_5) gives the equation

$$K_{sp} = 1.04058881 + 0.01194334t - 0.05323702(\%\ P_2O_5) + 0.00059789(\%\ P_2O_5)^2 - 0.00019269t(\%\ P_2O_5)$$

correlation coefficient $R^2 = 0.998$

coefficient of variation $CV = 3.21$ (6)

Again, the equation should only be used within the range of the experimental variables (40–55% P_2O_5 and 80–100 °C). Moderate extrapolations may be made using the van't Hoff relationship.

Glossary

R^2	correlation coefficient
CV	coefficient of variation
ΔH	apparent heat of solution at saturation
T	absolute temperature, K
R	gas constant, 1.987 cal K^{-1} mol^{-1}
C	integration constant
K_{sp}	solubility product constant, $(\%)^2$

Registry No. H_3PO_4, 7664-38-2; $CaSO_4 \cdot 0.5H_2O$, 10034-76-1.

Literature Cited

(1) Slack, A. V. *Phosphoric Acid*; Marcel Dekker: New York, 1968; Vol. 1, Part 1.
(2) Becker, P. *Phosphates and Phosphoric Acid*; Marcel Dekker: New York, 1983.
(3) Dahlgren, S. E. *J. Agric. Food Chem.* **1960**, *8* 411-412.
(4) Kelley, K. K.; Southard, J. C.; Anderson, C. T. U.S. Bureau of Mines Tech. Paper No. 625, 1941.
(5) Toy, A. D. F.; Walsh, E. N. *Phosphorus Chemistry in Everyday Living*; American Chemical Society: Washington, DC, 1987.
(6) Taperova, A. A. *Zh. Prikl. Khim.* **1940**, *13*, 643-651.
(7) Taperova, A. A.; Shul'gina, M. N. *Zh. Prikl. Khim.* **1945**, *18*, 521-528.
(8) Shpunt, S. Ya.; Shul'gina, M. N.; Guseva, Z. I. *Zh. Prikl. Khim.* **1967**, *40*, 1236-1242.
(9) Laptev, V. M.; Kopylev, B. A.; Varshavskii, B. A.; Ovsyanikova, L. G. *Sb. Tr.—Leningr. Tekhnol. Inst. im. Lensoveta* **1973**, *4*, 11-22.
(10) Daniels, F.; Mathews, J. H.; Williams, J. W.; Bender, P.; Alberty, R. A. *Experimental Physical Chemistry*; McGraw-Hill: New York, 1956.

Received for review November 12, 1987. Accepted February 29, 1988.

Solution Thermodynamics of First-Row Transition Elements. 1. Apparent Molal Volumes of Aqueous $NiCl_2$, $Ni(ClO_4)_2$, $CuCl_2$, and $Cu(ClO_4)_2$ from 15 to 55 °C

Randall Pogue and Gordon Atkinson*
Department of Chemistry, University of Oklahoma, Norman, Oklahoma 73019

We have used a flow densimeter to measure the densities of aqueous solutions of $NiCl_2$, $Ni(ClO_4)_2$, $CuCl_2$, and $Cu(ClO_4)_2$ at 10 °C intervals from 15 to 55 °C. Infinite dilution apparent molal volumes are determined at each temperature by using the Redlich–Meyer equation. These values are fitted to the polynomial $\phi_v^0 = a + bt + ct^2$. The Pitzer formalism has been used to fit the volume data over the entire concentration range (0–3.5 m).

Introduction

There are many practical situations in which it is desirable to know the densities of electrolyte solutions and how these densities are affected by changes in temperature. For example, there is a growing interest in the properties of concentrated electrolyte solutions and their application to industrial processes, the chemistry of geothermal brines, and oil well completion.

Most volume work has been done on solutions of single

0021-9568/88/1733-0370$01.50/0 © 1988 American Chemical Society

electrolytes and electrolyte mixtures at 25 °C. Much of this work was done with dilute solutions for the determination of the thermodynamically important ϕ_v^0. Comparatively little precision work has been done at high ionic concentrations. The situation worsens when you move away from 25 °C. In this paper, we present experimentally determined densities of $NiCl_2$, $Ni(ClO_4)_2$, $CuCl_2$, and $Cu(ClO_4)_2$ solutions from 15 to 55 °C at 10 °C intervals over a wide concentration range (0–3.5 m).

The apparent molal volumes (AMV) have been extrapolated to zero concentration to obtain the limiting values at infinite dilution, which are the same as the infinite dilution partial molal volumes. The Pitzer formalism is used to analyze the volume data over the entire temperature and concentration range. Finally, the conventional ionic partial molal volumes of the M^{2+}(aq) ions were calculated and the values compared to those obtained in previous work.

Experimental Section

The $NiCl_2$ and $CuCl_2$ were Fisher Scientific ACS certified. The perchlorates were prepared by saturating Mallinckrodt ACS certified perchloric acid with reagent grade $NiCO_3$ or $CuCO_3$. The perchloric acid was gently warmed to speed the reaction to completion. The resulting saturated solutions were cooled to room temperature and then gravity filtered with a 10-μm fritted filter to remove excess MCO_3 and crystalline $M(ClO_4)_2$. All solutions were prepared by using distilled water that was passed through a NANOPure (Barnstead 18.5 Mohm) ion-exchange apparatus.

The $NiCl_2$ and $CuCl_2$ stock solution concentrations were determined to within ±0.05% by gravimetric analysis of chloride. The stock solution M^{2+} concentrations were analyzed by EDTA titration as described by Schwarzenbach and Flaschka (*1*). These concentrations were determined to within ±0.07%. Solutions utilized in subsequent measurements were prepared by weight dilution of these stock solutions. The perchlorate stock solutions were kept slightly acidic with pH values between 4 and 5. This is necessary for two reasons. First, if the pH is too high, the hydrolysis of M^{2+} to MOH^+ will occur. Second, if the pH is too low, the contribution of $HClO_4$ to the solution properties is no longer negligible.

The solution densities were measured by a vibrating tube densimeter (Mettler/Paar, Model DMA 602); the theory of operation for vibrating tube densimeters has been previously described (*2*). A densimeter constant was obtained for each temperature by calibration with NaCl solutions using the density data of Perron et al. (*3*) and Chen et al. (*4*) in the concentration range up to 6 m. All measurements were made using the flow technique with solutions kept in a thermostated water bath controlled to ±0.005 °C. The absolute temperature was determined with a Leeds and Northrup platinum resistance thermometer (NBS standardized) and a Mueller bridge connected to a Leeds and Northrup dc null detector (Model 9828), yielding an accuracy of ±0.001 °C. The uncertainty in the period of the densimeter was 2 in 10^7 giving an uncertainty in the relative density of ±5 ppm. Characteristic vibration frequencies of the instrument with pure water were checked after every three to four solution measurements making it easy to spot and discard spurious solution data.

Results and Discussion

The apparent molal volume, ϕ_v, can be directly related to the solution densities, d, by the equation

$$\phi_v = M_2/d - 1000(d - d_0)/mdd_0 \quad (1)$$

where d_0 is the density of water, m is the molality of solution, and M_2 is the formula weight of the solute. Densities were calculated from the experimentally determined relative densities (RD) given in Table I, using the water densities of Kell (*5*). The corresponding values of ϕ_v are also listed in Table I.

The calculated apparent molal volume data was analyzed in two basic steps: (1) the dilute data points were fitted to a limiting law type of equation to extract ϕ_v^0 values, and (2) the entire data set was fitted to the Pitzer equation. The dilute apparent molal volume data ($m < 0.2$) were fitted to the Redlich–Meyer equation (*6*)

$$\phi_v = \phi_v^0 + S_v m^{1/2} + b_v m \quad (2)$$

where ϕ_v^0 is the value of ϕ_v at infinite dilution, S_v is the Debye–Hückel limiting slope, and b_v is an adjustable parameter.

The second step involved fitting the entire data set to the Pitzer equation. The Pitzer equation for the apparent molal volume of a single salt $M\nu_M X\nu_X$ is

$$\phi_v = \phi_v^0 + v|Z_M Z_X|A_v/2b \ln(1 + bI^{1/2}) + 2\nu_M\nu_X RT[mB^v_{MX} + m^2(\nu_M\nu_X)^{1/2}C^v_{mx}] \quad (3)$$

where

$$B^v_{MX} = \left(\frac{\partial\beta^{(0)}}{\partial P}\right)_T + \left(\frac{\partial\beta^{(1)}}{\partial P}\right)_T\left(\frac{2}{\alpha^2 I}\right)[1 - (1 + \alpha I^{1/2})\exp(-\alpha I^{1/2})] \quad (4)$$

$$C^v_{MX} = 0.5\left(\frac{\partial C^\phi}{\partial P}\right)_T \quad (5)$$

$$v = \nu_M + \nu_X \quad (6)$$

$$\alpha = 2.0\ (\text{kg/mol})^{1/2} \quad (7)$$

$$b = 1.2\ (\text{kg/mol})^{1/2} \quad (8)$$

$$A_v = \text{Debye–Hückel constant} \quad (9)$$

$$R = 83.1441\ \text{cm bar mol}^{-1}\ \text{K}^{-1} \quad (10)$$

The values of A_v used were those calculated in this laboratory (*7*): 1.715, 1.874, 2.055, 2.260, and 2.495 at 15, 25, 35, 45, and 55 °C, respectively.

The infinite dilution partial molal volumes of the salts were used to calculate conventional ionic values (based on $\bar{V}^0 = 0$ for H^+) for the transition metals. When measurements are made in dilute solutions, the instrument precision becomes important. The error in the measured apparent molal volume is a function of the uncertainty in solution molalities, solute formula weight, water density, period measurement, and temperature. The dominant source of error occurs in the period measurement which is proportional to $1/m$.

$$\sigma_{\phi_v} \approx (M_2/d^2 + 1000/md^2)^2(\sigma_d)^2 \quad (11)$$

where σ_d depends upon the uncertainty in the period measurements and temperature fluctuations. Error propagation calculations show a ±0.5 $cm^3\ mol^{-1}$ uncertainty at $m = 0.01$; this uncertainty escalates to 1.5 $cm^3\ mol^{-1}$ at $m = 0.005$. Using this criteria, we chose a limiting molality of 0.01.

The ϕ_v^0 values have been determined by fitting the dilute data to eq 2 by using a weighted nonlinear least-squares fit. Weighting was proportional to $1/\sigma_{\phi_v}$ (see eq 11). Figure 1 shows an example of the results obtained by this method and the resulting ϕ_v^0 values are listed in Table II. The values of ϕ_v^0 (M^{2+}) calculated from values of $\phi_v^0(Cl^-)$ and $\phi_v^0(ClO_4^-)$ (*8*) by using the additivity principle are given in Table III.

The values of $\phi_v^0(M^{2+})$ were determined independently from the chloride and perchlorate salts. These values deviated less

Table I. Relative Densities and AMV's of Aqueous Ni^{2+} and Cu^{2+} Solutions

molality, mol kg^{-1}	1000(RD), g cm^{-3}	ϕ_v, cm^3 mol^{-1}	molality, mol kg^{-1}	1000(RD), g cm^{-3}	ϕ_v, cm^3 mol^{-1}	molality, mol kg^{-1}	1000(RD), g cm^{-3}	ϕ_v, cm^3 mol^{-1}	molality, mol kg^{-1}	1000(RD), g cm^{-3}	ϕ_v, cm^3 mol^{-1}
					$NiCl_2$						
					288.15 °C						
0.00906	1.11	6.56	0.07449	9.08	7.49	0.600	70.97	10.45	1.9982	222.46	14.88
0.01948	2.39	6.70	0.1023	12.45	7.74	0.8003	93.79	11.24	2.5079	273.89	15.94
0.02981	3.65	6.80	0.2025	24.48	8.35	0.9881	114.77	11.96	2.9976	321.52	16.65
0.04910	6.00	7.19	0.3925	46.92	9.52	1.4970	170.24	13.50	3.3543	355.08	17.47
					298.15 °C						
0.01004	1.22	7.18	0.07527	9.09	8.41	0.5957	69.93	11.30	1.9982	220.95	15.36
0.01980	2.40	7.68	0.1023	12.32	8.70	0.7891	91.67	12.02	2.5075	271.96	16.41
0.02912	3.53	7.81	0.1997	23.90	9.35	0.9881	113.74	12.74	3.0023	319.63	17.34
0.04962	6.00	8.14	0.4045	47.84	10.52	1.4973	168.94	14.10	3.3543	352.70	17.89
					308.15 °C						
0.00906	1.09	7.69	0.07449	8.93	8.88	0.6000	69.87	11.70	1.9982	201.15	15.88
0.01947	2.35	7.91	0.1023	12.24	9.16	0.8003	92.33	12.47	2.5079	270.41	16.72
0.02975	3.59	8.24	0.2025	24.08	9.76	0.9881	113.06	13.06	2.9976	317.62	17.55
0.04911	5.91	8.54	0.3925	46.16	10.85	1.4970	187.19	14.47	3.3543	350.90	18.12
					318.15 °C						
0.00906	1.09	7.99	0.07520	8.97	9.12	0.6000	69.52	11.88	1.9982	210.07	16.03
0.01991	2.39	8.20	0.1026	12.21	9.40	0.8025	92.12	12.64	2.5186	270.23	16.87
0.03033	3.64	8.44	0.2025	23.95	10.01	0.9925	112.99	13.27	3.0275	319.15	17.68
0.04911	5.88	8.75	0.3925	45.98	11.01	1.4970	157.41	14.67	3.3595	349.68	18.28
					328.15 °C						
0.00977	1.18	8.26	0.07582	8.99	9.32	0.6012	69.27	12.05	1.9982	219.50	16.13
0.02005	2.39	8.44	0.1030	12.17	9.66	0.8043	91.78	12.83	2.5079	270.75	16.97
0.03209	3.82	8.64	0.2036	23.94	10.23	1.0032	113.56	13.43	2.9976	317.98	17.79
0.04935	5.87	8.93	0.3958	46.06	11.18	1.4970	167.98	14.82			
					$Ni(ClO_4)_2$						
					288.15 °C						
0.00640	1.29	56.21	0.04585	9.16	56.94	0.3893	75.49	59.09	1.5043	266.49	63.44
0.01259	2.52	56.44	0.07439	14.81	57.21	0.5765	110.14	59.83	1.9642	335.44	64.94
0.01875	3.76	56.57	0.1087	21.58	57.62	0.8068	151.24	60.82			
0.03236	6.28	56.77	0.2027	39.93	58.14	0.9764	180.53	61.49			
					298.15 °C						
0.01021	2.01	59.57	0.07611	14.90	60.52	0.6084	113.80	62.99	2.0350	340.44	67.15
0.02011	3.96	59.92	0.1086	21.17	60.86	0.8120	149.44	63.68	2.5565	411.10	68.38
0.03009	5.92	60.05	0.2012	38.94	61.28	1.0133	183.52	64.33	3.0676	475.10	69.46
0.05020	9.85	60.38	0.4078	77.54	62.24	1.5306	266.20	65.83	3.4232	516.73	70.16
					308.15 °C						
0.00640	1.24	61.89	0.07423	14.31	63.02	0.8068	146.28	65.95	1.7831	326.11	68.61
0.01259	2.44	62.22	0.1083	20.82	63.20	0.9764	174.77	66.33	1.9642	435.25	70.16
0.01867	3.62	61.39	0.2021	38.52	63.74	1.5043	258.57	67.70	2.8841	447.62	70.38
0.03122	6.05	62.53	0.3890	72.89	64.75	1.6773	284.60	67.97	3.4232	511.18	71.34
0.04585	8.87	62.67	0.5765	106.43	65.31						
					318.15 °C						
0.00640	1.22	65.82	0.07430	14.05	66.27	0.8068	144.01	68.19	1.9642	321.60	70.32
0.01259	2.39	65.98	0.1087	20.50	66.39	0.9764	172.04	68.54	2.7831	429.95	71.53
0.01875	3.56	65.97	0.2027	37.92	66.66	1.5043	254.70	69.57	2.8841	442.22	71.73
0.03136	5.95	66.01	0.3890	71.73	67.20	1.6773	280.69	69.71	3.4232	504.88	72.67
0.04585	8.69	66.10	0.5765	104.69	67.78						
					328.15 °C						
0.00640	1.20	67.48	0.04585	8.59	67.87	0.3890	70.91	68.77	1.5043	251.80	70.93
0.01259	2.36	67.61	0.07430	13.89	67.96	0.5765	103.58	69.13	1.6971	280.30	71.11
0.01875	3.52	67.67	0.1087	20.26	68.05	0.8062	142.26	69.67	1.9670	318.46	71.58
0.03136	5.88	67.84	0.2026	37.49	68.25	0.9764	170.08	69.98	2.7870	425.65	72.74
					$CuCl_2$						
					288.15 °C						
0.01027	1.27	9.85	0.07517	9.25	11.09	0.6119	72.38	14.99	1.9955	219.26	20.09
0.02113	2.62	9.97	0.09715	11.92	11.43	0.8038	94.00	15.91	2.4934	267.04	21.53
0.03040	3.76	10.41	0.2006	24.38	12.49	1.0333	119.31	16.78	2.9953	313.21	22.70
0.04879	6.02	10.71	0.3888	46.63	13.78	1.5005	168.92	18.64	3.5741	364.02	23.85
					298.15 °C						
0.01004	1.23	10.91	0.07493	9.10	12.48	0.6219	72.57	16.28	2.0791	224.36	21.45
0.02007	2.46	11.14	0.1003	12.16	12.63	0.8160	94.14	17.16	2.6006	273.22	22.89
0.03010	3.68	11.58	0.2006	24.10	13.66	1.0223	116.60	18.01	3.1291	321.30	23.87
0.05018	6.12	12.03	0.4130	48.82	15.19	1.5704	174.28	19.95	3.5741	360.18	24.59
					308.15 °C						
0.01027	1.25	12.08	0.03040	3.68	12.42	0.07517	9.07	13.02	0.2006	23.87	14.45
0.02113	2.57	12.37	0.04879	5.91	12.64	0.09715	11.69	13.30	0.3888	45.61	15.81

Table I (Continued)

molality, mol kg^{-1}	1000(RD), g cm^{-3}	ϕ_v, cm^3 mol^{-1}	molality, mol kg^{-1}	1000(RD), g cm^{-3}	ϕ_v, cm^3 mol^{-1}	molality, mol kg^{-1}	1000(RD), g cm^{-3}	ϕ_v, cm^3 mol^{-1}	molality, mol kg^{-1}	1000(RD), g cm^{-3}	ϕ_v, cm^3 mol^{-1}
0.6119	70.72	17.08	1.0333	116.52	18.92	1.9955	214.10	21.95	2.9953	306.09	24.34
0.8038	91.83	17.97	1.5005	164.92	20.60	2.4934	260.85	23.27	3.5741	355.92	25.39
					318.15 °C						
0.01027	1.24	12.05	0.07517	8.98	13.76	0.6119	69.85	18.06	1.9955	210.77	23.14
0.02113	2.55	12.61	0.09715	11.56	14.08	0.8038	90.45	19.25	2.4934	257.51	24.17
0.03040	3.65	13.01	0.2006	23.53	15.70	1.0333	114.59	20.33	2.9953	302.11	25.22
0.04879	5.85	13.42	0.3888	45.11	16.66	1.5005	162.39	21.82	3.5741	351.60	26.16
					328.15 °C						
0.01027	1.24	11.82	0.07517	8.94	13.81	0.6119	69.51	18.21	1.9955	209.34	23.45
0.02113	2.54	12.32	0.09715	11.53	14.11	0.8038	90.19	19.15	2.4934	255.01	24.74
0.03040	3.65	12.74	0.2006	23.51	15.38	1.0333	114.12	20.37	2.9953	299.34	25.73
0.04879	5.83	13.29	0.3888	44.89	16.81	1.5005	161.32	22.13	3.5741	348.21	26.70
					$Cu(ClO_4)_2$						
					288.15 °C						
0.01070	2.16	59.52	0.07109	14.30	60.22	0.6012	115.46	62.99	1.9972	343.09	67.43
0.02156	4.36	59.65	0.1073	21.52	60.45	0.7995	151.08	63.74	2.4893	411.97	68.60
0.03152	6.37	59.84	0.2166	42.98	61.22	1.0004	185.95	64.47	2.9743	474.99	69.61
0.05274	10.63	60.03	0.4059	79.25	62.16	1.4945	267.02	66.04	3.4994	538.36	70.55
					298.15 °C						
0.01020	2.02	63.35	0.1002	19.71	64.05	0.8036	149.17	66.54	2.4868	405.77	70.42
0.02014	3.99	63.52	0.1977	38.54	64.58	0.9873	180.50	67.16	3.0035	472.77	71.15
0.05092	10.06	63.72	0.4000	76.66	65.40	1.5013	263.69	68.44	3.4655	528.26	71.83
0.07688	15.16	63.89	0.6129	115.47	66.04	2.0084	339.54	69.50			
					308.15 °C						
0.01070	2.09	65.94	0.07109	13.79	66.68	0.6012	111.55	68.53	1.9972	333.38	71.20
0.02156	4.21	66.15	0.1073	20.76	66.79	0.7995	146.06	68.99	2.4893	401.06	71.94
0.03152	6.15	66.17	0.2166	41.44	67.51	1.0004	179.91	69.44	2.9743	463.19	72.59
0.05274	10.25	66.53	0.4059	76.51	68.03	1.4945	258.91	70.36	3.4994	525.83	73.22
					318.15 °C						
0.01070	2.05	68.99	0.07109	13.56	69.47	0.6012	109.74	71.00	1.9972	328.52	73.05
0.02156	4.13	69.15	0.1073	20.40	69.64	0.7995	143.71	71.37	2.4893	395.57	73.58
0.03152	6.03	69.30	0.2166	40.77	70.12	1.0004	177.16	71.61	2.9743	456.95	74.14
0.05274	10.08	69.34	0.4059	75.25	70.60	1.4945	254.88	71.46	3.4994	519.48	74.54
					328.15 °C						
0.01070	2.03	70.88	0.07109	13.39	71.41	0.6012	108.25	72.91	1.9972	324.37	74.55
0.02156	4.08	71.03	0.1073	20.14	71.54	0.7995	141.78	73.18	2.4893	391.28	74.79
0.03152	5.96	71.15	0.2166	40.26	71.95	1.0004	174.78	73.41	2.9743	452.09	75.28
0.05274	9.95	71.25	0.4059	74.24	72.55	1.4945	251.66	74.04	3.4994	513.90	75.66

Table II. Parameters for Eq 2

electrolyte	T, °C	ϕ_v^0, cm^3 mol^{-1}	b_v, cm^3 kg mol^{-2}	σ, cm^3 mol^{-1}
$Ni(ClO_4)_2$	15	55.58	−9.44	0.11
	25	58.65	−9.52	0.07
	35	61.04	−12.76	0.06
	45	64.66	−19.94	0.12
	55	66.30	−22.92	0.09
$NiCl_2$	15	5.67	−7.88	0.06
	25	6.39	−8.40	0.09
	35	6.60	−8.69	0.03
	45	6.66	−9.78	0.04
	55	5.98	−5.59	0.22
$CuCl_2$	15	8.90	−2.33	0.06
	25	10.07	−4.69	0.12
	35	10.85	−9.43	0.20
	45	11.12	−5.37	0.04
	55	10.76	−6.80	0.17
$Cu(ClO_4)_2$	15	58.52	−9.03	0.05
	25	62.29	−13.53	0.11
	35	64.82	−14.00	0.05
	45	67.79	−18.77	0.11
	55	69.49	−20.05	0.08

than ±0.2 cm^3 mol^{-1} at 25 °C, an error within experimental uncertainty. The two values were averaged yielding $\phi_v^0(Ni^{2+})$ = −29.37 cm^3 mol^{-1} and $\phi_v^0(Cu^{2+})$ = −25.71 cm^3 mol^{-1}. Our present values of $\phi_v^0(Ni^{2+})$ = −29.21 cm^3 mol^{-1} from $NiCl_2$ and $\phi_v^0(Ni^{2+})$ = −29.53 cm^3 mol^{-1} from $Ni(ClO_4)_2$ at 25 °C are in good agreement with the −29.5 cm^3 mol^{-1} value reported by

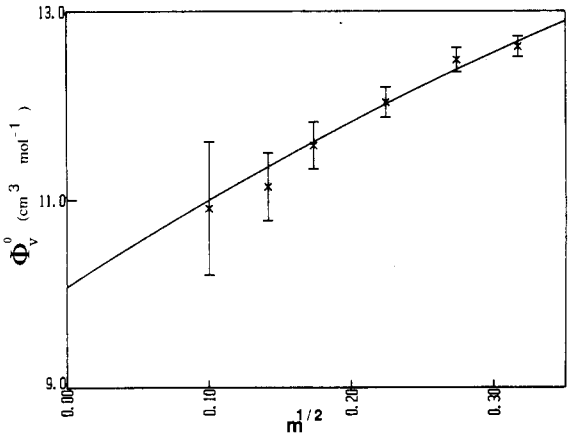

Figure 1. Plot of ϕ_v vs $m^{1/2}$ for $CuCl_2$ at 25 °C. Illustrates weighted NLLSQ fit with error bars indicating σ_{ϕ_v}.

Table III. Ionic Values of ϕ_v^0 from 15 to 55 °C

T, °C	$\phi_v^0(Cl^-)$, cm^3 mol^{-1}	$\phi_v^0(ClO_4^-)$, cm^3 mol^{-1}	$\phi_v^0(Ni^{2+})$, cm^3 mol^{-1}	$\phi_v^0(Cu^{2+})$, cm^3 mol^{-1}
15	17.12	42.20	−28.70 ± 0.13	−25.61 ± 0.27
25	17.80	44.09	−29.37 ± 0.16	−25.71 ± 0.18
35	18.00	45.52	−29.70 ± 0.30	−25.69 ± 0.54
45	17.99	46.62	−28.95 ± 0.37	−25.16 ± 0.30
55	17.74	47.56	−29.16 ± 0.34	−25.18 ± 0.45

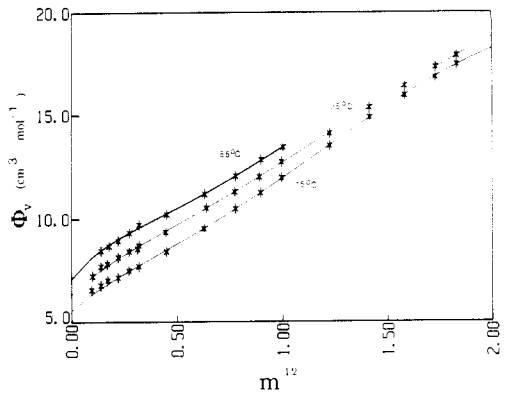

Figure 2. Plot of ϕ_v vs $m^{1/2}$ for $NiCl_2$ at 15, 25, and 55 °C showing the fit yielded by the Pitzer equation at each temperature.

Lo Surdo and Millero (*9*) and the −28.8 cm^3 mol^{-1} from Spitzer et al. (*10*). These values differ substantially from the −24.9 cm^3 mol^{-1} obtained from the $NiCl_2$ data of Kawaizumi et al. (*11*). The 25 °C values of $\phi_v^0(Cu^{2+})$ obtained from the chloride and perchlorate salt are −25.53 and −25.89 cm^3 mol^{-1}, respectively. Once again, these values compare favorably with the $\phi_v^0(Cu^{2+})$ = −25.5 cm^3 mol^{-1} obtained by Lo Surdo and Millero (*9*) and are slightly above the −25.1 and −24.3 cm^3 mol^{-1} reported by Spitzer et al. (*12*) and Kawaizumi et al. (*11*), respectively.

Comparison of limiting volumes at temperatures other than 25 °C becomes difficult due to limited data. The work done by Herrington et al. (*13*) at elevated temperatures yields results with similar trends to those found in this work. Comparison is somewhat difficult since the ϕ_v^0 values obtained by Herrington et al. were extrapolated from relatively concentrated solutions (0.3 *m*). The ϕ_v^0 values of Ni^{2+} and Cu^{2+} show only a slight temperature affect which is not significant enough to establish a trend. A comparison with the Ca^{2+} work done by Lo Surdo and Millero at varying temperatures with our data yields interesting results. The temperature change has similar affects on each cation; the ϕ_v^0 value changes approximately 1 cm^3 mol^{-1}. However, once again there seems to be no systematic temperature dependence.

The second stage of this work involved fitting the AMV data with a suitable theoretical equation for the entire concentration range. Initially, both a Pitzer and Brønsted–Güggenheim formalism were used to fit the volume data. Comparison of the fits obtained from each theory found the Pitzer fit to be superior to the Brønsted–Güggenheim for most of the salts. The form of the Pitzer equation shown in eq 3 was used with a weighted nonlinear least-squares fitting program. Three methods were used to try and fit the data. First, the ϕ_v^0 values listed in Table II were used and held constant while allowing $(\partial\beta^{(0)}/\partial P)_T$, $(\partial\beta^{(1)}/\partial P)_T$, and $(\partial C^\phi/\partial P)_T$ to vary, a three-parameter fit. Second, a two-parameter fit was utilized by setting $(\partial C^\phi/\partial P)_T$ = 0, while holding ϕ_v^0 constant. Finally ϕ_v^0, $(\partial\beta^{(0)}/\partial P)_T$, $(\partial\beta^{(1)}/\partial P)_T$, and $(\partial C^\phi/\partial P)_T$ were all used as adjustable parameters.

Graphical examination of the fits revealed that unnatural peculiarities occurred in the fits when ϕ_v^0 was held constant. These plots were distinguished by a "hump" in the low-concentration data. The fits obtained when $(\partial C^\phi/\partial P)_T$ = 0 were also unsatisfactory. These plots did not fit the concentrated portions of the data sets. Examination of the standard deviations lends support to these observations. We have chosen the final option which allows ϕ_v^0 to vary. The ϕ_v^0 values obtained from the analysis are strictly fitting parameters; the true ϕ_v^0 values were determined previously. This method allowed us to successfully fit the volume data at all concentrations and temperatures (see Figure 2). Table IV lists the Pitzer parameters for the four salts at each temperature.

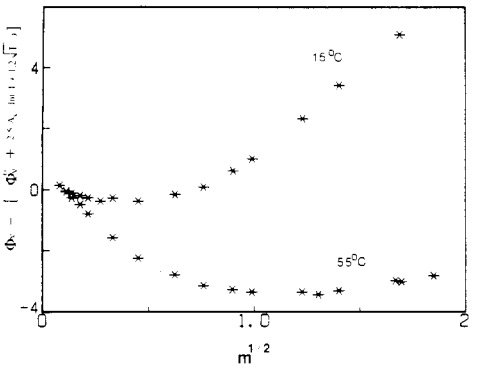

Figure 3. Plot of (ϕ_v − first term) vs $m^{1/2}$ for $Ni(ClO_4)_2$ at 15 and 55 °C showing the temperature dependence of the high-concentration terms in the Pitzer equation.

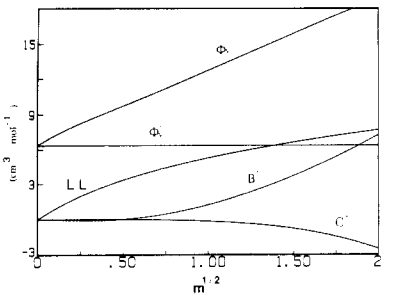

Figure 4. Concentration dependence of each Pitzer term; dilute LL, the intermediate concentration B^v, and the concentrated C^v term, for $NiCl_2$ at 25 °C.

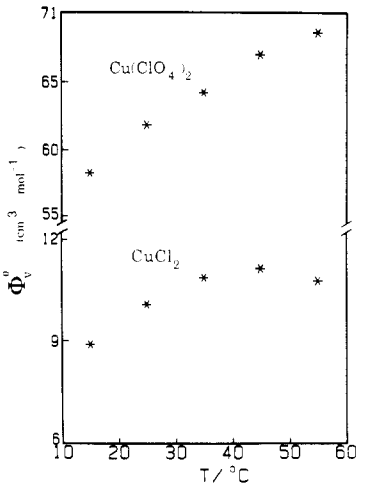

Figure 5. Temperature dependence of ϕ_v^0 for $CuCl_2$ and $Cu(ClO_4)_2$.

Figure 3 shows a plot of [ϕ_v − first term] vs $m^{1/2}$, where first term is the limiting portion of the Pitzer equation

$$\text{first term} = \phi_v^0 + v|Z_M Z_X|A_v/2b \ln(1 + bI^{1/2}) \quad (12)$$

The resulting plot illustrates the temperature dependence of the higher concentration terms. This dependence results in the terms having trends of opposite sign at 15 and 55 °C. Figure 4 shows the relative importance of the three terms in the Pitzer equation: the limiting Debye–Hückel term, the intermediate concentration term B^v, and the high-concentration term C^v. We see that at molalities greater than one the B^v and C^v terms' contribution to the total ϕ_v value becomes significant. At a solute molality of 4.0 these terms begin to dominate the limiting term. Consequently, we report two important trends. First, the high-concentration terms are significant. Second, the different terms show substantial temperature effects. Similar trends are observed for all four salts. A temperature dependence is also

Table IV. Parameters for Pitzer Equation

T, K	ϕ_v^0, cm^3 mol^{-1}	$10^5(\partial\beta^{(0)}/\partial P)_T$, kg mol^{-1} atm^{-1}	$10^5(\partial\beta^{(1)}/\partial P)_T$, kg^2 mol^{-2} atm^{-1}	$10^6(\partial C^\phi/\partial P)_T$, kg^2 mol^{-2} atm^{-1}
		$NiCl_2$		
288.15	5.57 ± 0.07	2.81 ± 0.10	−6.19 ± 1.01	−3.84 ± 0.30
298.15	6.35 ± 0.05	2.06 ± 0.08	−5.51 ± 0.76	−2.23 ± 0.25
308.15	6.73 ± 0.11	2.16 ± 0.15	−9.34 ± 1.56	−3.15 ± 0.47
318.15	6.88 ± 0.09	1.97 ± 0.14	−11.98 ± 0.13	−2.89 ± 0.45
328.15	7.07 ± 0.11	2.25 ± 1.09	−17.03 ± 4.00	−5.64 ± 0.86
		$Ni(ClO_4)_2$		
288.15	55.69 ± 0.05	3.52 ± 0.22	−14.78 ± 0.42	−3.69 ± 0.78
298.15	58.83 ± 0.03	2.20 ± 0.11	−13.18 ± 0.81	−1.67 ± 0.34
308.15	61.07 ± 0.04	1.09 ± 0.12	−10.56 ± 0.91	0.13 ± 0.36
318.15	64.67 ± 0.08	0.65 ± 0.20	−21.17 ± 1.63	0.39 ± 0.64
328.15	66.38 ± 0.06	0.89 ± 0.15	−27.53 ± 1.19	−1.35 ± 0.46
		$CuCl_2$		
288.15	8.93 ± 0.04	3.18 ± 0.07	1.37 ± 0.65	−3.49 ± 0.21
298.15	10.10 ± 0.07	3.12 ± 0.12	−1.59 ± 1.15	−4.18 ± 0.37
308.15	10.57 ± 0.09	2.63 ± 0.14	−0.17 ± 1.33	−3.21 ± 0.41
318.15	11.08 ± 0.16	2.30 ± 0.27	2.54 ± 2.48	−3.25 ± 0.81
328.15	10.73 ± 0.11	2.61 ± 0.17	−1.17 ± 1.64	−4.06 ± 0.54
		$Cu(ClO_4)_2$		
288.15	58.54 ± 0.03	2.89 ± 0.05	−10.47 ± 0.51	−3.44 ± 0.17
298.15	62.30 ± 0.06	2.00 ± 0.10	−15.52 ± 0.98	−2.69 ± 0.32
308.15	64.90 ± 0.06	0.81 ± 0.09	−13.88 ± 0.85	−0.44 ± 0.27
318.15	67.83 ± 0.06	0.41 ± 0.11	−19.14 ± 0.99	−0.45 ± 0.36
328.15	69.47 ± 0.07	−0.27 ± 0.14	−17.90 ± 1.18	0.56 ± 0.42

Table V. Parameters for Eq 12

	A, cm^3 mol^{-1}	B, cm^3 mol^{-1} deg^{-1}	C, cm^3 mol^{-1} deg^{-2}
$NiCl_2$	3.78	0.157	−0.0021
$CuCl_2$	6.04	0.227	−0.0026
$Ni(ClO_4)_2$	50.44	0.357	−0.0012
$Cu(ClO_4)_2$	52.29	0.458	−0.0026

observed in the ϕ_v^0 values. Figure 5 illustrates the temperature dependence of $\phi_v^0(CuCl_2)$ and $\phi_v^0(Cu(ClO_4)_2)$. Typical behavior is observed in all the salt systems, the ϕ_v^0's increase with temperature eventually reaching a maximum. The temperature maximum occurs in the $CuCl_2$ system at 44 °C. The $Cu(ClO_4)_2$ system indicates the existence of a maximum somewhere above 55 °C. The Ni^{2+} salts behave in a similar fashion. The ϕ_v^0 data was fitted to the equation

$$\phi_v^0 = A + Bt + Ct^2 \quad (13)$$

where t is the temperature in degrees Celsius. The resulting parameters are listed in Table V. It is useful to examine the temperature dependence of ϕ_v^0 to further describe the properties of these aqueous solutions. We obtain an equation for the partial molal expansibility by differentiating eq 13 with respect to temperature:

$$\phi_E^0 = \left(\frac{\partial\phi_v^0}{\partial T}\right)_P = B + 2Ct \quad (14)$$

It must be noted that the results yielded by eq 14 are twice removed from the experimental data. The quality of the expansibility data will be greatly dependent upon good volume data.

The temperature dependence of ϕ_v^0 can be looked at in terms of ionic hydration. Raising the temperature has the effect of decreasing ionic hydration which is reflected in the greater solute ϕ_v^0 values. This trend continues until the temperature is high enough to start breaking down the bulk solution structure. We see the maximum in ϕ_v^0 occur as the structure-making hydration effects become lost in the structure-breaking thermal effects in the bulk solvent. A second effect on the ϕ_v^0 values of $CuCl_2$ is due to ion pairing. Increased ion pairing causes the removal of water molecules from the primary hydration sphere

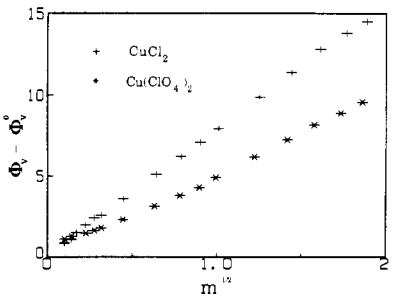

Figure 6. Plot of $(\phi_v - \phi_v^0)$ vs $m^{1/2}$ for $CuCl_2$ and $Cu(ClO_4)_2$ at 25 °C. Illustrates the effect of ion pairing on ϕ_v.

of the ions. These molecules then become part of the less ordered and less dense bulk solvent causing a net increase in volume. The significance of ion pairing in $CuCl_2$ has been calculated by using K_a values from Smith and Martell (*14*). Rough calculations at 25 °C reveal that 42% of the Cu^{2+} is present as $CuCl_x$ (x = 1, 2, ...) at $m(CuCl_2)$ = 0.2. This value increases to 88% at $m(CuCl_2)$ = 3.5. Figure 6 illustrates the effect of ion pair formation at high $CuCl_2$ concentrations. The quantity $(\phi_v - \phi_v^0)$ has been plotted for a non-ion-pair former, $Cu(ClO_4)_2$, and the $CuCl_2$ system at 25 °C. The positive deviation found in the $CuCl_2$ data indicates ion pair formation. A similar plot for $NiCl_2$ yielded only a slight positive deviation indicative of much less ion pairing. It is noted that ion pairing increases with temperature and we would expect this effect to become much larger at higher temperatures.

Registry No. $NiCl_2$, 7718-54-9; $Ni(ClO_4)_2$, 13637-71-3; $CuCl_2$, 7447-39-4; $Cu(ClO_4)_2$, 13770-18-8.

Literature Cited

(1) Schwarzenbach, G.; Flaschka, H. *Complexometric Titrations*; translated by H. M. N. H. Irving; Methuen: London, 1969.
(2) Picker, P.; Tremblay, E.; Jolicoeur, C. *J. Solution Chem.* **1974**, *3*, 377.
(3) Perron, G.; Roux, A.; Desnoyers, J. *Can. J. Chem.* **1981**, *59*, 3049.
(4) Chen, C. T.; Chen, L. S.; Millero, F. *J. Acoust. Soc. Am.* **1978**, *63*, 1795.
(5) Kell, G. *J. Chem. Eng. Data* **1975**, *20*, 97.
(6) (a) Redlich, O.; Meyer, D. M. *Chem. Rev.* **1964**, *64*, 221. (b) Redlich, O. *J. Phys. Chem.* **1963**, *67*, 496.
(7) Ananthaswamy, J.; Atkinson, G. *J. Chem. Eng. Data* **1984**, *29*, 81.
(8) Pogue, R.; Atkinson, G., unpublished results.
(9) Surdo, A. L.; Millero, F. J. *J. Phys. Chem.* **1980**, *84*, 710.

(10) Spitzer, J. J.; Singh, P.; Olofsson, I.; Hepler, L. J. Solution Chem. 1978, 7, 623.
(11) Kawaizumi, F.; Nomura, H.; Nakao, F. J. Solution Chem. 1987, 16, 133.
(12) Spitzer, J. J.; Singh, P.; McCurdy, K.; Hepler, L. J. Solution Chem. 1978, 7, 81.
(13) Herrington, T.; Roffey, M.; Smith, D. J. Chem. Eng. Data 1986, 31, 221.
(14) Smith, R. M.; Martell, A. E. Critical Stability Constants. Volume 4. Inorganic Complexes; Plenum: New York, 1976.

Received for review October 8, 1987. Accepted February 24, 1988. This work was supported by the Department of Energy under grant De-FG01-87FE61146.

Vapor–Liquid Equilibria at 760 mmHg in the Ternary System Methanol–Propyl Bromide–Methyl Methacrylate

Jaime Wisniak* and Abraham Tamir

Department of Chemical Engineering, Ben-Gurion University of the Negev, Beer Sheva, Israel 84105

Vapor–liquid equilibrium at atmospheric pressure has been determined for the title ternary system. The data were correlated by various equations and the appropriate parameters are reported.

The present work was undertaken to measure VLE data for the ternary system methanol–propyl bromide–methyl methacrylate for which no isobaric data are available. Data for the binary systems methanol–propyl bromide and propyl bromide–methyl methacrylate have been reported elsewhere (*1*, *2*) and thermodynamically consistent isobaric data for the system methanol–methyl methacrylate have been reported by Pavlov et al. (*3*). This work is part of a program to determine the UNIFAC parameters for organic bromides.

Experimental Section

Purity of Materials. Analytical grade methanol (99.5%+) was purchased from Frutarom, propyl bromide (99.4%) from Merck, and methyl methacrylate analytical grade (99.4%+) from Fluka. The reagents were used without further purification after gas chromatography failed to show any significant impurities. Properties of the pure components appear in Table I.

Apparatus and Procedure. An all-glass modified Dvorak and Boublik recirculation still (*4*) was used in the equilibrium determination. The experimental features have been described in previous publications (*5*). All analyses were carried out by gas chromatography on a Packard-Becker Model 417 apparatus provided with a thermal conductivity detector and a Spectra Physics Model SP 4290 electronic integrator. The column was 200 cm long and 0.2 cm in diameter, was packed with 20% OV-17, and was operated isothermally at 100 °C. Injector and detector temperatures were 220 and 230 °C, respectively. Very good separation was achieved under these conditions, and calibration analyses were carried to convert the peak ratio to the weight composition of the sample. Concentration measurements were accurate to better than ±1%. The accuracy in determination of pressure and temperature was $\Delta P = \pm 2$ mmHg and $\Delta t = \pm 0.02$ °C.

Results

The temperature–concentration measurements at 760 mmHg for the ternary system are reported in Table II together with the activity coefficients which were calculated from the following equation (*6*)

$$\ln \gamma_i = \ln(Py_i/P_i^0x_i) + (B_{ii} - V_i^L)(P - P_i^0)/RT + (P/2RT)\sum\sum y_j y_k(2\delta_{ji} - \delta_{jk}) \quad (1)$$

where

$$\delta_{ji} = 2B_{ji} - B_{jj} - B_{ii} \quad (2)$$

Table I. Physical Constants of Pure Components

index	compd	refractive index	bp(760 mmHg), °C	purity (GLC(min)), %
1	methanol	1.3280[a] (20 °C)	64.68[a]	99.5
		1.32840[b]	64.70[b]	
2	propyl bromide	1.4348[a] (20 °C)	70.55[a]	99.6
		1.4343[b]	71.0[b]	
			70.80[c]	
3	methyl methacrylate	1.4118[a] (25 °C)	100.4[a]	99.4
		1.4120[b]	100.3[b]	

[a] Measured. [b] Reference *13*. [c] Reference *14*.

Vapor pressures P_i^0 were calculated according to Antoine's equation

$$\log P_i^0 = \alpha_i - \beta_i/(\delta_i + t) \quad (3)$$

where the constants are reported in Table III. The molar virial coefficients B_{ii} and the molar mixed coefficient B_{ij} were calculated by the method of Tsonopoulos (*7*) using the molecular parameters suggested by the same author.

The ternary data reported in Table II were found to be thermodynamically consistent as tested by the McDermot–Ellis two-point method (*8*) modified by Wisniak and Tamir (*9*). Two experimental points a and b, at almost the same temperature, are considered thermodynamically consistent if the following condition is fulfilled:

$$D_{ab} < D_{max} \quad (4)$$

The local deviation D_{ab} is given by

$$D_{ab} = \sum_{i=1}^{N}(x_{ia} + x_{ib})(\ln \gamma_{ib} - \ln \gamma_{ia}) \quad (5)$$

where N is the number of components and the maximum local deviation D_{max} is

$$D_{max} = \sum_{i=1}^{N}(x_{ia} + x_{ib})(1/x_{ia} + 1/y_{ia} + 1/x_{ib} + 1/y_{ib})\Delta x + 2\sum_{i=1}^{N}|\ln \gamma_{ib} - \ln \gamma_{ia}|\Delta x + \sum_{i=1}^{N}(x_{ia} + x_{ib})\Delta P/P + \sum_{i=1}^{N}(x_{ia} + x_{ib})\beta_i\{(t_a + \delta_i)^{-2} + (t_b + \delta_i)^{-2}\}\Delta t \quad (6)$$

The errors in the measurements Δx, ΔP, and Δt were as previously indicated. The first term in eq 6 was the dominant one.

The activity coefficients were correlated by the following Redlich–Kister expansion (*10*)

$$\ln \gamma_1 = x_2x_3[(E_{12} + E_{13} - E_{23}) + F_{12}(2x_1 - x_2) + F_{13}(2x_1 - x_3) + 2F_{23}(x_3 - x_2) + G_{12}(x_1 - x_2)(3x_1 - x_2) + G_{13}(x_1 - x_3)(3x_1 - x_2) - 3G_{23}(x_3 - x_2)^2 + F_1(1 - 2x_1)] + x_2^2[E_{12} + F_{12}(3x_1 - x_2) + G_{12}(x_1 - x_2)(5x_1 - x_2)] + x_3^2[E_{13} + F_{13}(3x_1 - x_3) + G_{13}(x_1 - x_3)(5x_1 - x_3)] \quad (7)$$

0021-9568/88/1733-0376$01.50/0 © 1988 American Chemical Society